



STABILITY OF SLENDER WALL BOUNDARIES UNDER NON-UNIFORM STRAIN PROFILES

P.F. Parra⁽¹⁾, J.P. Moehle⁽²⁾

⁽¹⁾ Assistant Professor, School of Engineering and Sciences, Universidad Adolfo Ibáñez, Santiago, Chile, pablo.parra@uai.cl

⁽²⁾ Professor, Dept. of Civil and Environmental Engineering, University of California, Berkeley, CA 94720, U.S.A., moehle@berkeley.edu

Abstract

Prior 2010, out-of-plane instability in slender boundary elements subjected to cyclic loading had been observed in some experimental tests conducted on columns and walls but not in an actual earthquake. Later, buckling in slender walls was reported following the 2010 Chile and the 2011 New Zealand earthquakes. Structural walls have proved to be an effective system for the protection of buildings from strong earthquakes, and their design and use over the past decades has evolved in thinner and heavily stressed cross sections, which has pushed the boundaries for design to a critical point. Researchers have proposed in the past theoretical models for buckling of prismatic columns under uniform tension/compression cycles, where the key parameter is the maximum tensile strain prior buckling during load reversal. These models have shown good accuracy in comparison with experimental and analytical studies conducted on cyclically loaded columns under constant axial force. However, analysis of slender walls requires considering other aspects that influence the response. Walls have strain gradients along their length and height, and both effects must be considered for a more accurate estimation of the onset of out-of-plane instability. In some cases, the assumption of uniform axial strain along the wall height is reasonable. However, in the more general case, this assumption leads to an underestimation of the maximum tensile strain required to buckle the wall during load reversal and therefore to an overestimation of the minimum wall thickness required for design to prevent buckling from occurring. Moreover, the strain gradient along the wall length must also be considered for analysis. This paper presents the main findings of analytical studies conducted on isolated boundary elements and walls using two-dimensional nonlinear finite element models and nonlinear beam-column elements with force-based formulation, for the determination of the influence of the strain gradient along the wall length and height in the onset of out-of-plane instability. A simplified approach that can be used for pre-design purposes is proposed to evaluate the onset of out-of-plane instability in a variety of cases.

Keywords: stability; buckling; slenderness; wall; earthquake

1. Introduction

In the past, structural walls typically had enlarged boundary elements that prevented global instability in boundary elements during seismic loading. In recent years, walls are constructed with rectangular sections or interconnected rectangles, and enlarged boundary elements are seldom used in many countries. Today, it is not uncommon to find in many countries walls with thickness 6 to 8 in. (150 to 200 mm), resulting in floor-to-floor slenderness of $h_w/b = 16$ or even greater.

Prior 2010, out-of-plane buckling of columns and structural walls during cyclic loading had been reported only in a few laboratory tests (Oesterle et. al [1]; Goodsir [2]; Chai and Elayer [3]; Thomsen and Wallace [4]) but not in an actual earthquake. In 2010, following the Mw 8.8 Maule Earthquake, out-of-plane buckling of slender walls was reported in two buildings in Chile (Parra and Moehle [5]; ATC-94 [6]). Damage associated with out-of-plane deformation of structural wall boundaries was also observed following the Mw 7.1 New Zealand Earthquake in 2011 (Sritharan et al [7]). These observations created a renewed interest in the practical aspects of inelastic buckling of slender structural walls.

The capabilities of finite element models in predicting nonlinear behavior and failure patterns of reinforced concrete walls, including global instability, has been investigated (Dashi et. al [8]). More recently, wall tests have confirmed that in-plane flexure may cause global instability in slender walls (Rosso et. al [9]).



(a)

(b)

Fig. 1 – Global instability in slender wall boundaries: a) building in Chile after the 2010 earthquake (DICTUC [10]); b) buckled specimen during wall test (Rosso et. al [9])

The onset of global instability in slender walls is believed to depend not only on the flexural-compression force acting on the boundary elements but also on the magnitude of the tensile strain experienced by the wall boundary prior loading in the opposite direction (Paulay and Priestley [11]; Chai and Elayer [3]; Parra and Moehle [5]). This is because residual tensile strains in the previously yielded longitudinal reinforcement leave the wall boundary with open cracks, and during crack closure any asymmetry may cause out of plane curvature and instability.



2. Relevant Code Requirements for Wall Slenderness

Provisions governing the slenderness of structural walls designed as compression members are contained in Chapter 11 of ACI 318-14 [12]. According to section 11.3.1, for a given unsupported wall height, h_u , an empirical method limits wall slenderness ratios to $h_u/b \leq 25$, and corresponding wall thicknesses to $b \geq 4$ inches, in which b is the thickness of the extreme flexural compression fiber. Alternatively, walls can be designed by section 11.5.2 or analyzed by 11.8 of ACI 318-14, in which case there are no minimum thickness requirements.

Previously, the Uniform Building Code (1997) [13] required $h_u/b \leq 16$ for structural walls providing lateral resistance in regions of highest seismicity. This provision was intended to ensure lateral stability for wall boundaries. This provision was not carried forward into the International Building Code (2000) [14] and subsequent editions.

Up through its 2011 edition, ACI 318 did not limit the slenderness of special structural walls, that is, walls intended to provide lateral force resistance in buildings assigned to the highest seismic design categories. However, the 2014 edition of ACI 318 introduced slenderness provisions for such walls. According to section 18.10.6.4(b), where special boundary elements are required, the width of the flexural compression zone, b , along the special boundary element region, including flange if present, shall be at least $h_u/16$. This is a new requirement of ACI 318-14 introduced to prevent lateral instability failures of slender wall boundaries observed in recent earthquakes (Parra and Moehle [5]; ATC-94 [6]). For walls with large cover, where spalling of cover concrete would lead to a significantly reduced section, ACI 318-14 recommends considering a larger thickness for the boundary element.

ACI 318-14, section 11.7.2.3 requires two curtains of reinforcement for walls thicker than 10 inches. Additionally, section 18.10.2.2 requires at least two curtains of reinforcement in walls having a factored design shear force $V_u > 2A_{cv}\lambda\sqrt{f'_c}$ or $h_w/l_w \geq 2$ where h_w and l_w refer to height and length of the entire wall, A_{cv} is the web area (equal to wall length, l_w , times wall web thickness, b_w), λ is a modification factor for lightweight aggregate concrete, and f'_c is the specified compressive strength of the concrete (psi). Otherwise one curtain of reinforcement is permitted. These provisions are intended to improve stability of wall boundaries.

Eurocode 8 (2004) [15] specifies minimum wall thickness of 8 inches (200mm) for confined parts of walls. Moreover, if the length of the confined part does not exceed the larger of $2b$ and $0.2l_w$, b must be at least $h_u/15$. Otherwise, b must be at least $h_u/10$.

3. Global Instability in Prismatic Columns under Uniform Tension/Compression Cycles

Parra and Moehle [5] introduced a relation between the critical slenderness ratio and the maximum tensile strain prior to compressive load, ϵ_{sm} . This relation was derived from the mechanics of instability in prismatic columns under uniform tension/compression cycles. Eq. (1) presents this relation.

$$\frac{b_{cr}}{kh_u} = \frac{1}{\pi} \sqrt{\frac{\epsilon_{sm} - 0.005}{\kappa\xi}} \quad (1)$$

where κ is a factor for the effective depth for out-of-plane bending of the member and kh_u is the effective length of the member in the direction of instability. Eq. (2) shows the inequality that relates the parameter ξ with the mechanical reinforcement ratio, $m = \rho f_y / f'_c$.

$$\xi \leq 0.5 \left(1 + \frac{2m}{0.85} - \sqrt{\left(\frac{2m}{0.85}\right)^2 + \frac{4m}{0.85}} \right) \quad (2)$$

The parameters of Eq. (1) are inconvenient for pre-design purposes, and typical values can be adopted for these parameters in order to simplify the expression ($\kappa \approx 0.8$ for members with two curtains of reinforcement and $\sqrt{\xi} = 0.5$ for practical construction). Therefore, Eq. (1) becomes:

$$\frac{b_{cr}}{kh_u} = 0.7\sqrt{\epsilon_{sm} - 0.005} \quad (3)$$

Chai and Elayer [3] tested fourteen prismatic columns using axial reversed cyclic tension/compression load. These data are relevant because in those tests the tensile and compressive strains were gradually increased until overall buckling occurred. All specimens had pin-ended boundary conditions ($k = 1$). Fig. 2 compares the results of Eq. (3) with the observed points at onset of overall lateral instability.

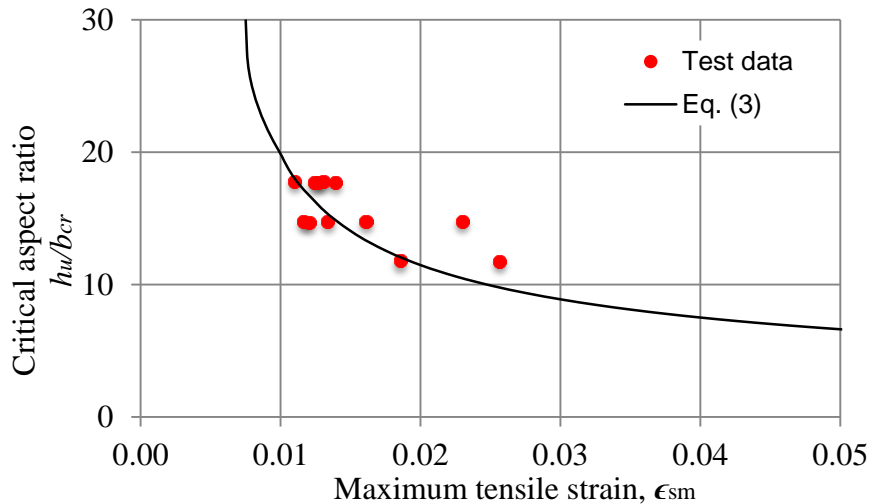


Fig. 2 – Comparison between Eq. (3) and experimental data, after Parra and Moehle [5]

The results suggest that Eq. (3) is a reasonable approximation to describe behavior of uniformly loaded prisms.

4. Global Instability of Boundary Elements in Slender Walls

The derivation of Eq. (1) is based on a prismatic column subjected to tension/compression cycles, where the axial force and strain are uniform along the column height (more details in Parra and Moehle [5]). Fig. 2 showed that this model is a reasonable approximation of uniformly loaded slender columns.

Fig. 3 depicts two walls in a multistory building, with their corresponding moment diagram over the height. Each diagram intends to represent the typical case of a wall that interacts with a frame. For the first wall of Fig. 3(a), the moment variation over the first story height is small enough to be neglected, and therefore the assumption of constant axial force/strain over the height of the corresponding boundary element seems to be reasonable. For this case, if the influence of the strain profile along the wall length is not considered as a first approach, Eq. (1) can be used to estimate the tensile strain required to trigger lateral instability during load reversal. For the second wall of Fig 3(b), the moment variation over the first story cannot be neglected, and Eq. (1) may lead to an unacceptable underestimation of the tensile strain needed to buckle the element or, in other words, to an unacceptable overestimation of the critical slenderness to prevent buckling if the tensile strain demand is known (Parra [16]).

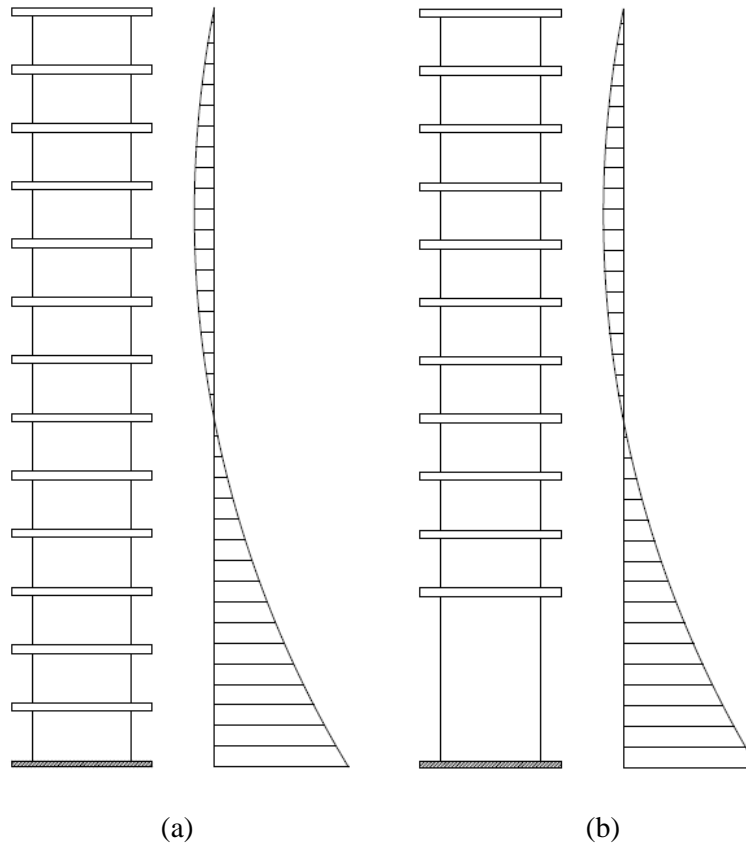


Fig. 3 – Moment variation over the height in multistory wall: a) negligible moment gradient over the first story height, b) non negligible moment gradient over the first story height, after Parra [16]

The influence of force/strain gradients along the wall length and height are now studied separately. The effect of the force/strain variation along the height of isolated boundary elements is evaluated using force-based nonlinear beam-column elements with fibers in OpenSees, as shown in Fig. 4. A corotational formulation is considered to include nonlinear geometry, and a specific axial force diagram is obtained from the application of vertical point forces at the nodes, considering that the current corotational transformation in OpenSees does not allow to use element forces. The force variation is intended to represent the variation of the flexural compression force and tension force over wall height due to the presence of a moment gradient.

Several axial force diagrams are considered to evaluate how the variation of the axial force over the height affects the onset of out-of-plane instability in isolated boundary elements under cyclic loading.

Regarding the support conditions, the boundary element is fixed at the base, and the rotation and horizontal displacements are restrained at the top. The boundary elements were analyzed considering incremental tension and compression cycles until reaching buckling failure during load reversal.

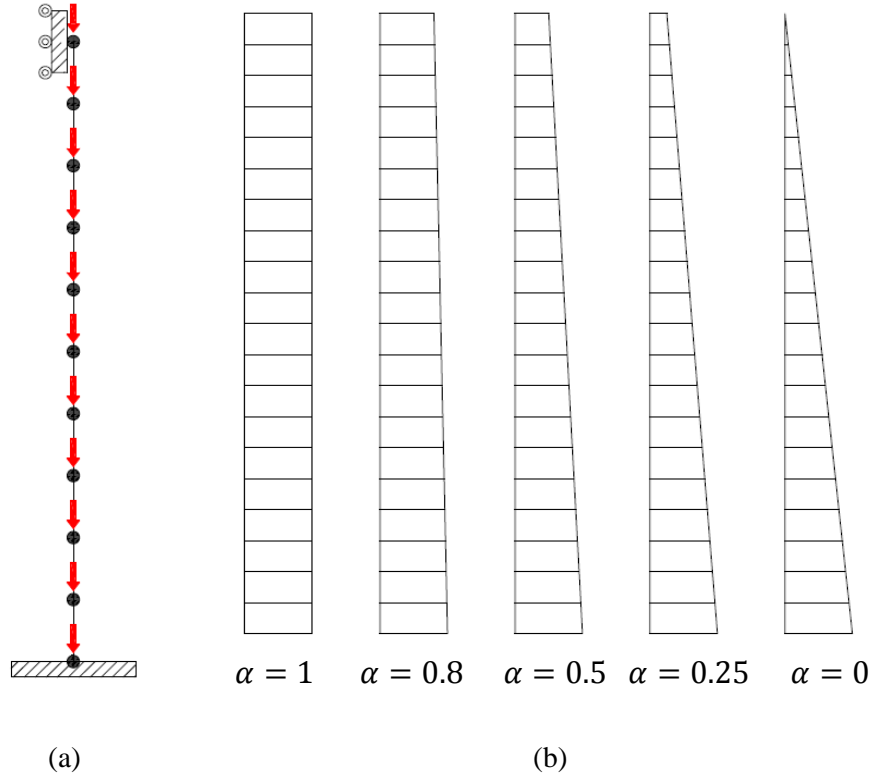


Fig. 4 – Slender wall boundary element: a) OpenSees model with ten force-based elements; b) axial force gradients, after Parra [16]

Five isolated boundary elements are analyzed considering the axial force profiles of Fig. 4(b) and an effective length factor $k=0.5$ for fixed support conditions: slenderness $kh_u/b=14.75$ with longitudinal reinforcement ratio $\rho=2.1\%$ and $\rho=3.8\%$, $kh_u/b=17.75$ with $\rho=2.1\%$ and $\rho=3.8\%$, and finally an element of slenderness $kh_u/b=25$ with $\rho=2.1\%$. All of them have rectangular cross section of 4x8 in. (102x203mm). The first four cases correspond to the columns specimens tested by Chai and Elayer [3]. Material properties for modeling were also obtained from the same source. The parameter α represents the variation of the axial force along the element height, and it is defined as the ratio of the axial force at the top of the element to the axial force at the base of the element.

Fig. 5 and 6 present some analysis results for the element with slenderness $kh_u/b=14.75$ and longitudinal reinforcement ratio $\rho=2.1\%$. Parra and Moehle [5] assumed a sine function for the buckled shape of a prismatic column under uniform tension/compression cycles, and this theoretical out-of-plane displacement (normalized by its maximum value) is compared with the results obtained from OpenSees modeling for several axial force profiles in Fig. 5. Fig. 6 shows the strain demand along the element height at the point of maximum tensile strain prior buckling during load reversal, normalized by the yielding strain of the reinforcement bars, for several axial force profiles.

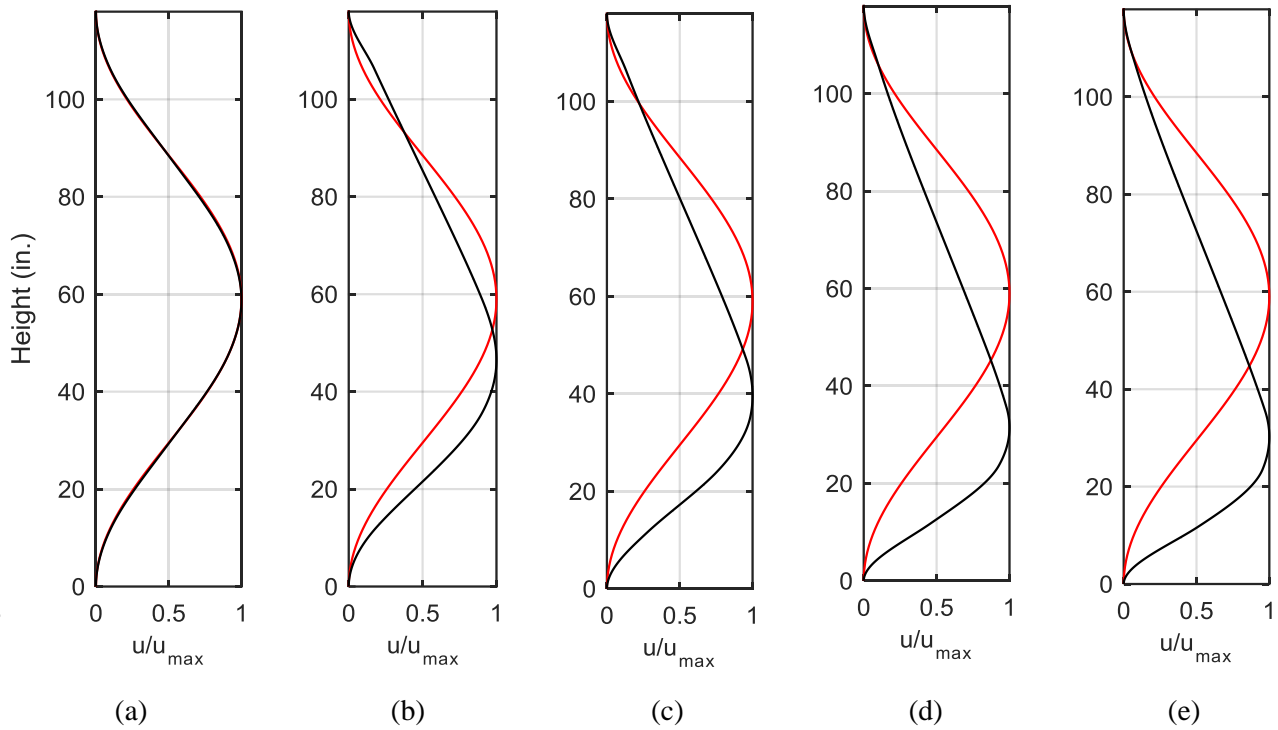


Fig. 5 – Normalized out-of-plane displacement, theoretical shape (in red) versus OpenSees modeling ($kh_u/b = 14.75$, $\rho = 2.1\%$) for: a) uniform axial force profile $\alpha = 1$; b) $\alpha = 0.8$; c) $\alpha = 0.5$; d) $\alpha = 0.25$; e) $\alpha = 0$, after Parra [16]

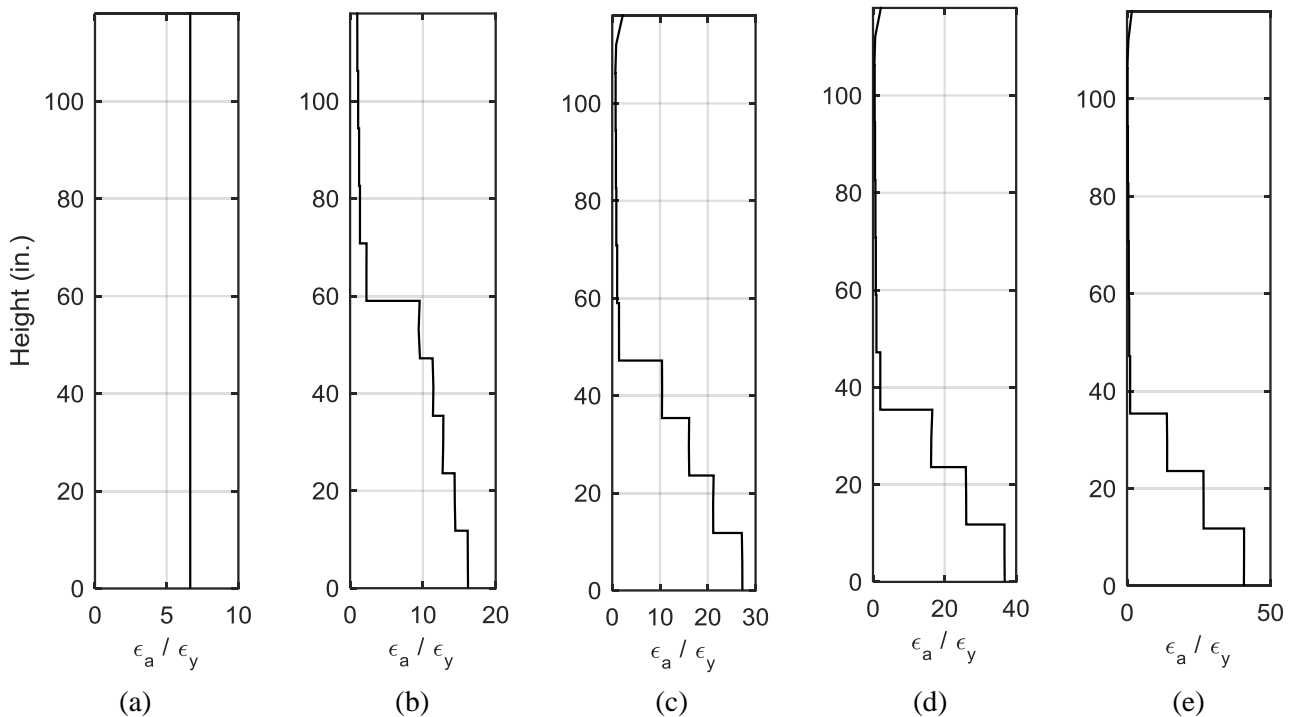


Fig. 6 – Normalized tensile strain profile, prior buckling during load reversal, along the element height ($kh_u/b = 14.75$, $\rho = 2.1\%$) from OpenSees modeling for: a) uniform axial force profile $\alpha = 1$; b) $\alpha = 0.8$; c) $\alpha = 0.5$; d) $\alpha = 0.25$; e) $\alpha = 0$, after Parra [16]

From Fig. 5(a), for the case of uniform axial force profile ($\alpha = 1$), the buckled shape obtained from OpenSees matches the sine shape used by Parra and Moehle [5] in the development of their buckling theory. Fig. 6(a) shows that the maximum tensile strain prior buckling during load reversal for this case is $7\epsilon_y$ or 0.013. This value is constant along the element height and very close to 0.012, value obtained from Eq. (1), which is an expected result considering that the theoretical model assumes cycles of uniform tension/compression. The measured value of tensile strain prior buckling for this specimen (Chai and Elayer [3]) was 0.016.

When the axial load changes to a non-uniform profile, the buckled shape obtained from analysis does not correspond to the theoretical buckled shape assumed in the derivation of the simplified mechanics (Fig. 6(b) to (e)), and the point of maximum lateral displacement moves towards the element base as the α value decreases. For the case of triangular axial force profile shown in Fig. 6(e), the point of maximum out-of-plane displacement is located at 30 in. (0.76 m) from the element base, which is 25% of the total element height.

Moreover, when the axial force profile is non-uniform, the axial strain demand over the element height is also not constant. Fig. 6(b) to (e) show that the maximum tensile strain prior buckling that occurs at the element base increases when the α value decreases. For this case, when the axial force profile is uniform, it is required to reach a tensile strain of $7\epsilon_y$ to buckle the element during load reversal, and this value increases up to $45\epsilon_y$ if the axial force profile is triangular ($\alpha = 0$). This is almost 7 times the strain required when the axial force is uniform. This behavior was also observed in the other four boundary elements analyzed (Parra [16]).

According Eq. (1), the most important demand parameter for the evaluation of the onset of out of plane instability is the maximum tensile strain prior buckling during load reversal. This value has been theoretically and experimentally obtained for uniformly loaded prisms (Chai and Elayer [3]) and now has been analytically obtained for several axial load profiles, demonstrating that the results of the simplified theory are over-conservative for cases where the assumption of constant axial force/strain over the height is not valid.

Fig. 7 shows the maximum tensile strain prior buckling normalized by the corresponding value for uniform force over the height ($\alpha = 1$) versus α , the parameter that represents the axial force profile (previously defined as the axial force at the top divided by the axial force at the base of the element). For the analyzed cases, which correspond to very slender walls with typical steel ratios at boundary elements between 2% and 4%, it is proposed to use a linear relation between the ratio $\epsilon_{sm}/\epsilon_{sm(\alpha=1)}$ and α (Parra [16]). This ratio can be used to improve the estimation of the maximum tensile strain prior buckling obtained from the simplified mechanics (Eq. 1), now considering a non-uniform stress profile along the boundary element height.

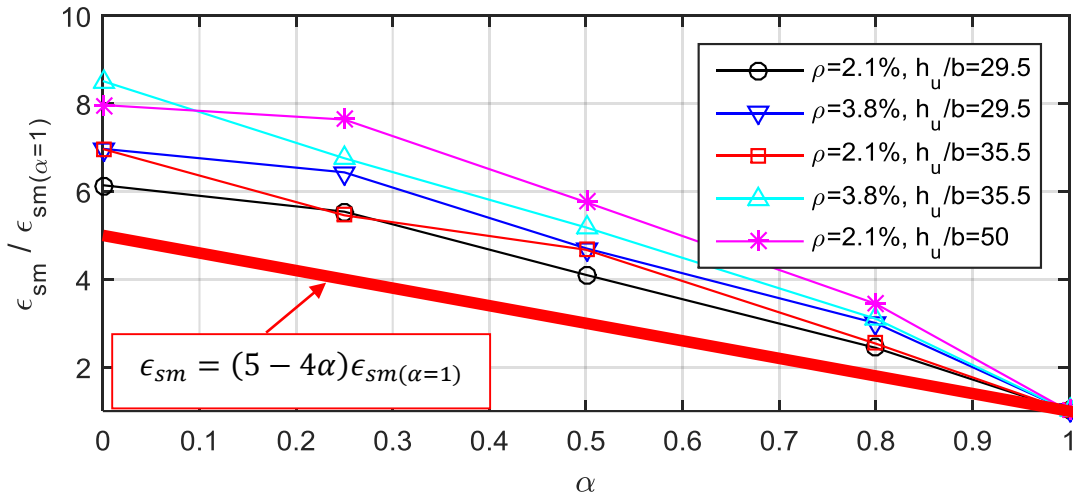


Fig. 7 – Maximum tensile strain prior buckling during load reversal, normalized by the corresponding value for uniform axial force profile, versus α , after Parra [16]

For example, consider a boundary element with slenderness $kh_u/b = 15$, subjected to an axial force demand that can be approximated by linear profile with $\alpha = 0.2$. From Eq. (3), the maximum tensile strain required to buckle the element during load reversal, under the assumption of uniform tension/compression cycles, is $\epsilon_{sm} = 0.014$. It has been shown that this is an over-conservative estimation of the required tensile strain for a case where

the gradient of axial force over the element height cannot be neglected. From Fig. 7, for $\alpha = 0.2$ the value of ϵ_{sm} should be amplified by $(5 - 4\alpha) = 4.2$ to obtain a more reasonable approximation of the required tensile strain prior buckling, which is $\epsilon_{sm} = 0.014 \cdot 4.2 = 0.06$.

In order to study the influence on instability of the gradient of the vertical strains along the wall length, the response of an isolated boundary element is compared with the response of corresponding walls (identical boundary elements details) of different lengths. The use of force-based nonlinear beam-column elements in OpenSees for buckling analysis presented previously is limited to axially loaded columns (or isolated boundary elements). In walls, buckling is a more complicated phenomenon because it occurs locally at the boundary elements and does not necessarily propagate through the entire cross section. Therefore, the use of a single beam-column element located at the centroid of the cross section cannot accurately represent the complex behavior expected in a wall boundary. Two-dimensional nonlinear finite element models can be used to perform buckling analysis in walls. These models allow representing the local buckling expected in wall edges more accurately. For this case, the software TNO DIANA [17] is used to perform nonlinear finite element analysis in buckled specimens. Geometric nonlinearity is considered using a Total Lagrange description. Four-node, quadrilateral isoparametric curved shell elements (Q20SH) are selected. These elements are based on an isoparametric degenerated-solid approach by introducing two shell hypotheses: straight normal and zero normal stress. The first hypothesis assumes plane sections remain plane but not necessarily orthogonal to the reference surface (it includes shear deformation according to Reissner-Mindlin theory). The second hypothesis assumes that the normal stress component in the normal direction of a lamina basis is forced to zero. This formulation allows using several integration points within the element thickness, which is fundamental for buckling modeling. In TNO DIANA, longitudinal reinforcing bars can be modeled as embedded reinforcement, which means that the bars do not have degrees of freedom of their own and their strains are computed from the displacement field of the mother elements. Therefore, there is perfect bond between the reinforcement and the surrounding concrete. In this formulation the finite element mesh can be defined independently of the bar locations. In this study, the smeared crack model is used for concrete (Rashid [18]; Feenstra [19]), where the cracked solid is considered as a continuum. Therefore, the behavior of cracked concrete is described in terms of stress-strain relations and, upon cracking, the initial stress-strain relation is replaced by an orthotropic stress-strain relation. The finite element mesh is then preserved, which makes this model computationally efficient. The concrete constitutive model is based on a total strain concept. For this study, the rotating crack model embedded in a total strain concept is used, and the uniaxial stress-strain relationship considered for concrete in tension is linear tension softening ultimate strain based. A parabolic fracture-energy dependent curve is used for concrete compressive behavior. The modeling of shear behavior is only necessary in the fixed crack approach. Therefore, it is not considered in this study. For reinforcement bars, the uniaxial Giuffrè-Menegotto-Pinto material with isotropic strain hardening is used (Filippou et al [20]).

Fig. 8 presents a typical wall cross section, where the boundary elements details were obtained from the prismatic columns tested by Chai and Elayer [3].

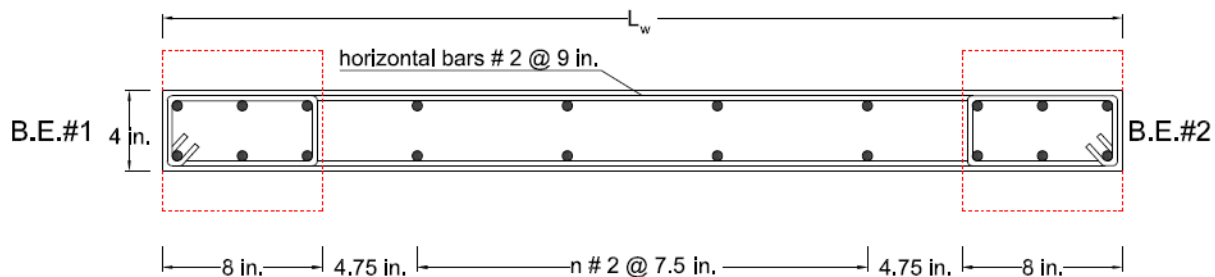


Fig. 8 – Reinforcement details in typical cross section, after Parra [16]

Translations in the direction orthogonal to the wall plane and the corresponding rotations are restrained at the top and bottom to represent the wall continuity expected in a typical multistory wall. The objective of this study is to determine the maximum tensile strain, caused by in-plane flexure, required to buckle the boundary element during load reversal. Analyses of walls of several lengths provide valuable information regarding the

influence of the location of the neutral axis on the onset of lateral instability. Cyclic moments that cause incremental tensile strain and no compressive strain in the boundary element 1 (B.E. #1) are applied until reaching buckling in that edge during crack closure.

Fig. 9 shows six buckled walls, all of them with boundary elements of slenderness $kh_u/b = 14.75$ and longitudinal reinforcement ratio $\rho = 2.1\%$, geometry obtained from one of Chai and Elayer specimens. A detailed description of all the analyzed cases can be found elsewhere (Parra [16]), and only some results obtained for walls of Fig. 9 are discussed here. These walls were subjected to a uniform vertical strain profile over the boundary element height and variable strain profile over the wall length caused by in-plane flexure.

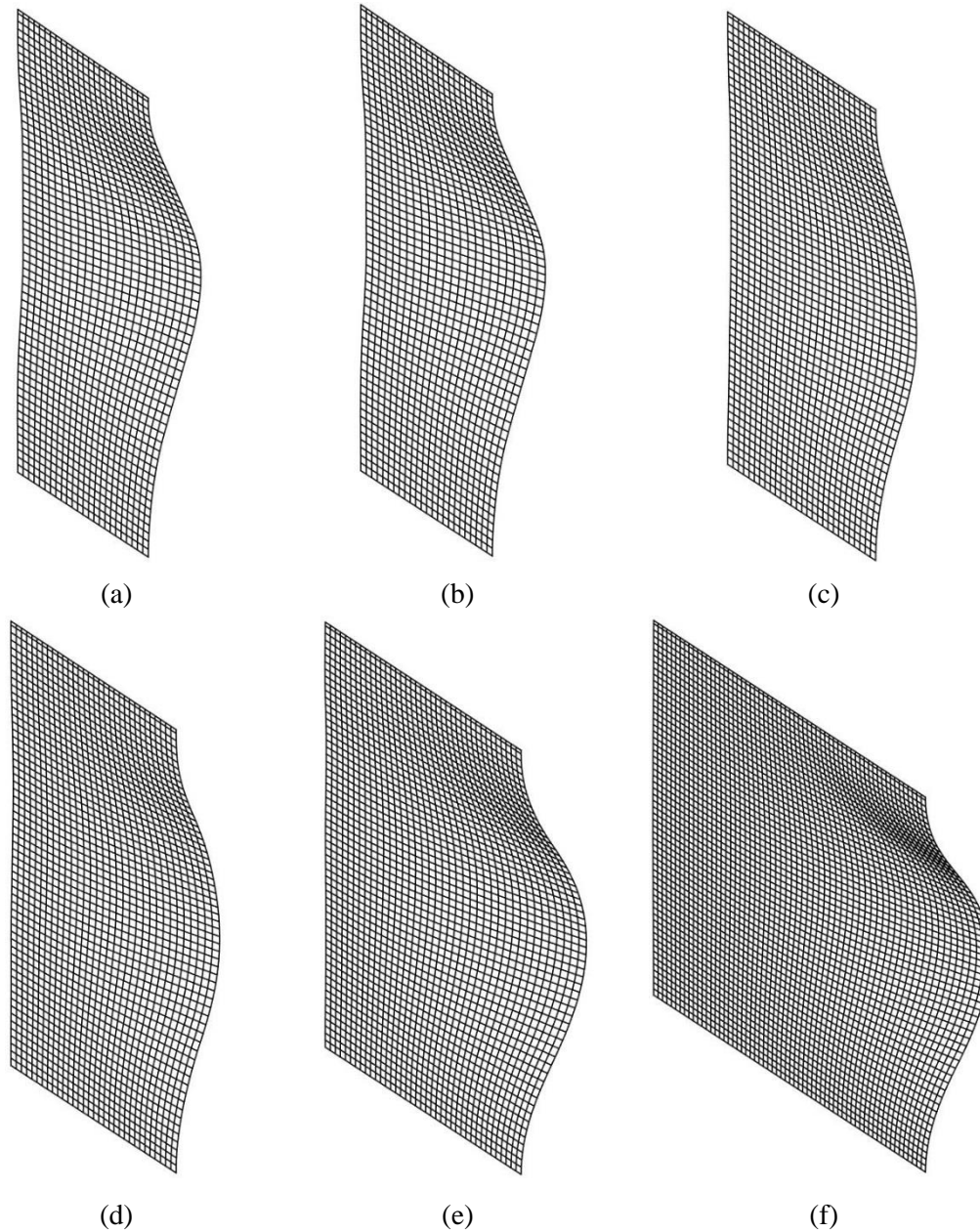


Fig. 9 – Buckled walls with slenderness $kh_u/b = 14.75$, longitudinal reinforcement ratio at boundary elements $\rho = 2.1\%$ and different lengths of: a) 41 in. (1 m); b) 48 in. (1.2 m); c) 56 in. (1.4 m); d) 63 in. (1.6 m); e) 78 in. (2 m); f) 123 in. (3.1 m), after Parra [16]



For all the cases shown in Fig. 9, when the maximum tensile strain at the wall edge prior buckling is reached, the extension of the compression zone in the wall is small, that is, almost the entire cross section is in tension. The extension of the tension zone for the analyzed cases ranges from 10 to 30 times the wall thickness. Analysis results show that in walls where the axial force is constant over the boundary element height with tension zones extending along the wall a length exceeding 10 times the wall thickness, the value of the maximum tensile strain at the boundary element prior buckling, ϵ_{sm} , is almost insensitive to the location of the neutral axis. For the six analyzed cases, this value is close to $5\epsilon_y$, which is the value calculated for the isolated boundary element in OpenSees.

Out-of-plane displacements obtained for each wall show that there is not a specific portion of the wall where the lateral displacement concentrates. Lateral instability involves a significant length of the wall in all cases. Analysis results suggest that the maximum tensile strain prior buckling ϵ_{sm} is more influenced by the axial force distribution along the boundary element height rather than the variation of vertical strain along the wall length, for tension zones longer than 10 times the wall thickness, which is a typical case in real buildings. Other cases analyzed by Parra [16] support this observation.

5. Conclusions

Prior 2010, lateral buckling of slender wall boundaries had been observed only in laboratory tests but not in actual buildings subjected to earthquake shaking. The 2010 Chile earthquake showed that buckling is a potential risk to slender walls that should be considered in the design process.

The tendency of an intact wall to buckle under cyclic loading depends not only on the aspect ratio h_u/b of the wall boundary but also on the maximum tensile strain experienced by the member prior to axial compression.

A simplified mechanics model (Parra and Moehle [5]) for buckling of prismatic sections under uniform tension/compression cycles provides a good estimate of the conditions required to initiate buckling of uniformly loaded prisms.

Analytical studies using finite elements and nonlinear beam/column elements were conducted to determine the effects on wall boundary instability of (a) strain gradients along the wall length and (b) strain/moment gradients along the wall height. These studies showed that the effect of the gradient along the length can be neglected for walls longer than 10 times the wall thickness, which is the typical case of walls prone to buckle. The strain gradient along the height can have an important effect of improving the stability of the wall boundary.

In typical multistory buildings, the assumption of uniform strain along the unsupported height at the first story is often reasonable, and in such cases the onset of out-of-plane instability can be identified using expressions derived from the simplified mechanics model. In some special cases, the moment gradient over the unsupported height can influence the buckling tendency of a wall in a building. In such buildings, the assumption of uniform axial demand over the height can lead to an underestimation of the maximum tensile strain required to buckle the boundary element during load reversal. The effects of moment gradient should be considered in such cases. A correction factor is introduced for that purpose.

6. Acknowledgements

This research has been supported by the National Institute of Standards and Technology through the ATC 94 project. Opinions, findings, conclusions and recommendations are those of the writers and do not necessarily represent those of the sponsor. The first author would like to thank Comisión Nacional de Investigación Científica y Tecnológica (CONICYT, Chile) and the Fulbright Student Program, for providing necessary financial assistance to support this research, and the School of Engineering and Sciences of Universidad Adolfo Ibáñez, for providing the required funding for the participation in the 16th World Conference on Earthquake Engineering.



7. References

- [1] Oesterle, R.G., Fiorato, A.E., Johala, L.S., Carpenter, J.E., Russell, H.G., Corley, W.G. (1976): Earthquake resistant of structural walls – tests of isolated walls, Report to National Science Foundation, Portland Cement Association, Construction Technology Laboratories, Skokie.
- [2] Goodsir, W.J. (1985): The design of coupled frame-wall structures for seismic actions, *Research report 85-8*, Department of Civil Engineering, University of Canterbury, Christchurch, New Zealand.
- [3] Chai, Y.H., Elayer, D.T. (1999): Lateral stability of reinforced concrete columns under axial reversed cyclic tension and compression, *ACI Structural Journal*, American Concrete Institute, V. 96, No. 5, pp. 780-789.
- [4] Thomsen, J.H., Wallace, J.W. (2004): Displacement-based design of slender reinforced concrete structural walls-experimental verification, *J. Struct. Eng.*, 130(4), 618-630.
- [5] Parra, P.F., Moehle, J.P. (2014): Lateral buckling in reinforced concrete walls, *Proceedings of the 10th National Conference in Earthquake Engineering*, Earthquake Engineering Research Institute, Anchorage, AK.
- [6] ATC-94 (2014): Recommendations for seismic design of reinforced concrete wall buildings based on studies of the 2010 Chile earthquake, Applied Technology Council, Redwood City, California.
- [7] Sritharan, S., Beyer, K., Henry, R. S., Chai, Y. H., Kowalsky, M., & Bull, D. (2014): Understanding poor seismic performance of concrete walls and design implications, *Earthquake Spectra*, 30(1), 307-334.
- [8] Dashti, F., Dhakal, R., Pampanin, S. (2014): Numerical simulation of shear wall failure mechanisms, *2014 NZSEE Conference*, Auckland, New Zealand, New Zealand Society for Earthquake Engineering.
- [9] Rosso, A., Almeida, J. P., Beyer, K. (2015): Stability of thin reinforced concrete walls under cyclic loads: state-of-the-art and new experimental findings, *Bulletin of Earthquake Engineering*, 1-30.
- [10] DICTUC (2010): Contrastación de la existencia en terreno de elementos de confinamiento de borde y del plano de algunos muros versus especificaciones de planos estructurales tras sismo del 27 de febrero de 2010. *Report # 878055*, Santiago, Chile.
- [11] Paulay, T., Priestley, M.J.N. (1993): Stability of ductile structural walls, *ACI Structural Journal*, V. 90, No. 4, pp. 385-392.
- [12] ACI 318 (2014): Building code requirements for structural concrete (ACI 318-14) and commentary (ACI 318R-14), American Concrete Institute, Farmington Hills, MI.
- [13] UBC (1997): Uniform building code, International Conference of Building Officials, Whittier, CA.
- [14] IBC (2000): International building code, International Conference of Building Officials, Whittier, CA.
- [15] Eurocode 8 (2004): Design of structures for earthquake resistance, Part 1, European Committee for Standardization, Brussels.
- [16] Parra, P.F. (2015): Stability of reinforced concrete wall boundaries, Ph.D. Dissertation, University of California, Berkeley.
- [17] TNO DIANA (2011): Finite element analysis user's manual-release 9.4.4.
- [18] Rashid, Y.R. (1968): Ultimate strength analysis of prestressed concrete pressure vessels, *Nuclear Engineering and Design*, 7(4): 334-344.
- [19] Feenstra, P.H., De Borst, R., Rots, J.G. (1991): A comparison of different crack models applied to plain and reinforced concrete, *Fracture Processes in Concrete, Rock and Ceramics*, pp. 629–638.
- [20] Filippou, F. C., Popov, E. P., & Bertero, V. V. (1983): Effects of bond deterioration on hysteretic behavior of reinforced concrete joints. *Tech. Rep. EERC 83-19*, Earthquake Engineering Research Center, University of California, Berkeley.